PREDICTION OF THE BEHAVIOR OF ELASTOPLASTIC ROADS DURING REPEATED ROLLING USING THE MECHANO-LATTICE ANALOGY

W. O. Yandell, School of Highway Engineering, University of New South Wales, Sydney

Repeated axial load triaxial tests on a road material are described. They showed that the plasticity of an elastoplastic road material decreases more with repeated loading than with continuous loading. When the cell pressure is high the damping factor and the elastic compliances also decrease more rapidly. The initial elastoplastic characteristics of a road material were ascribed to a hypothetical pavement being repeatedly traversed by a rigid roller and by a pneumatic tire respectively. The author's mechano-lattice analogy was used to calculate the transient and residual stress patterns after each of six passes. The distribution of horizontal flow of the hypothetical pavement was calculated by the same means. These theoretical findings compared qualitatively with the results of corresponding laboratory tests. It was shown that a maximum residual stress is attained, in this case, after six rolling passes and that the road material flows forward against the direction of traffic movement in a complicated but predictable manner. It is thought that the flow behavior may contribute to the growth of uneveness on road surfaces.

•APART from the author's previous work (1, 2, 3), some useful predictions of subgrade stress-strain behavior have been made. The predictions are for stationary pavement loads only, and they fall into two classes: (a) when the subgrade material is able to consolidate on a temporal basis and (b) where the subgrade is assumed to obey the linearized theory of elasticity. The assumptions that were made, however, rendered both classes unrealistic in view of the large nonelastic components of strain in pavements and subgrades, particularly under construction and fluctuating moisture conditions. The effect of stress-strain hysteresis is also neglected.

This paper describes the author's triaxial tests (2) involving the measuring of the damping and stress-strain properties of a road material subjected to a large number of repeated axial loads. It is shown how these results can be used with the author's mechano-lattice analogy to predict the instantaneous and residual stress and plastic strain behavior in a hypothetical pavement subjected to repeated rolling.

REPEATED-LOAD TRIAXIAL TESTS

Apparatus

It is difficult to produce in a test sample the precise stress-strain regime that a road material is likely to sustain under the action of passing traffic. Triaxial conditions, rotating axes of principal stress, and cyclically varying major, minor, and intermediate principal stresses all must be capable of being controlled and varied in a realistic laboratory material test. In the tests described here and reported earlier (4, 5), a compromise was made between instrumentation difficulties and reality of test conditions.

Sponsored by Committee on Compaction.

A triaxial testing machine, in which the axial load could be applied and removed with a constant rate of strain once a minute, was used. The adjustable cell pressure was held constant during a test involving 10,000 load applications. A number of sequences of readings, recorded by automatic photography, were distributed on a logarithmic basis throughout the period of a test. The cyclic and permanent axial and volumetric deflections and corresponding fluctuating loads were recorded. Stress-strain hysteresis loops were plotted from each sequence of readings, and a damping factor equal to the area in the loop divided by the area under the loading curve was calculated.

Tests

Tests are described to demonstrate how repeated loading can change the stress-strain characteristics of a road material. A 2 x 2 x 3 factorial experiment was carried out on a mixture of 50 percent kaolin and 50 percent sand with a moisture content of 12.4 percent. An X-ray diffractogram of the kaolin revealed 20 percent ground quartz, 50 percent kaolinite, 5 percent illite, 15 percent mixed layer minerals, and 10 percent montmorillonite. Two levels of cell pressure (5 psi and 40 psi), two levels of saturation (dry densities of 118 and 124.6 pcf—98 percent saturated), and three levels of repeated axial stress (52, 62, and 72 percent of the ultimate strength) were used. The ultimate strength was taken as the stress at 18 percent axial strain. A nuclear method was used to check the uniformity of compaction of the samples.

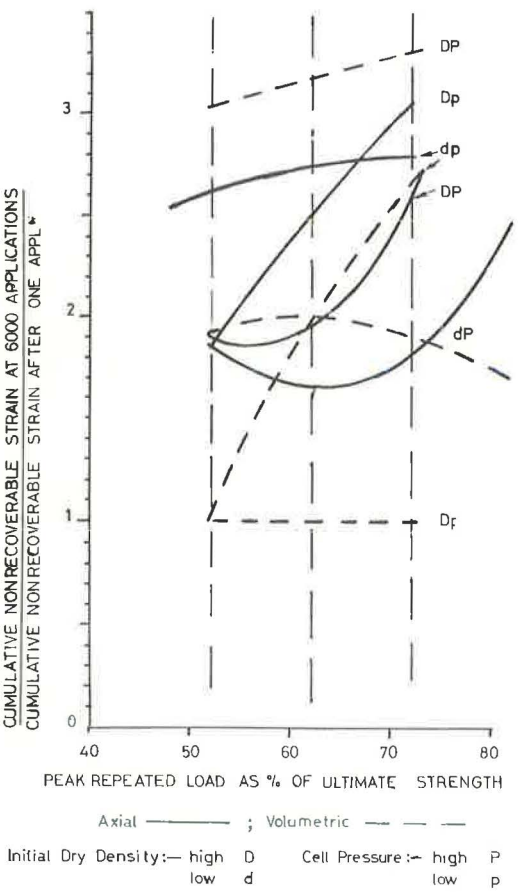

Figure 1. Ratio of cumulative plastic strain after 6,000 load applications over that after one application versus the magnitude of repeated loads.

Results

Figure 1 shows the ratio of the cumulative plastic strain after 6,000 cycles of load over that after one cycle versus the magnitude of the repeated load. It can be seen that axial plastic deformation increased with repeated loading, especially when the cell pressure was low. However, Figure 2 shows the typical manner in which the rate of increase in cumulative plastic deformation gradually decreased until it almost ceased at a high number of load cycles. This demonstrates how a subgrade becomes more stable with the number of load applications or with time when loaded. Creep tests (4) have shown that repeating the load is not very much more effective than holding the load constant in effecting this gradual reduction in plasticity. The saturation increased during the tests, as is evident from the increase in dry density.

The Young's chord moduli of the samples under low cell pressure did not increase greatly with repeated loading, as is shown in Figure 3. The increase in rigidity when the cell pressure was high resulted from the greater consolidation of the samples under high hydrostatic pressures.

The damping factor influences rolling resistance and, when the hysteresis loops are open, can indicate plastic deformation. As shown in Figure 4, it decreased with repeated loading; more so when the cell pressure was high. The increased consolidation under high cell pressures may

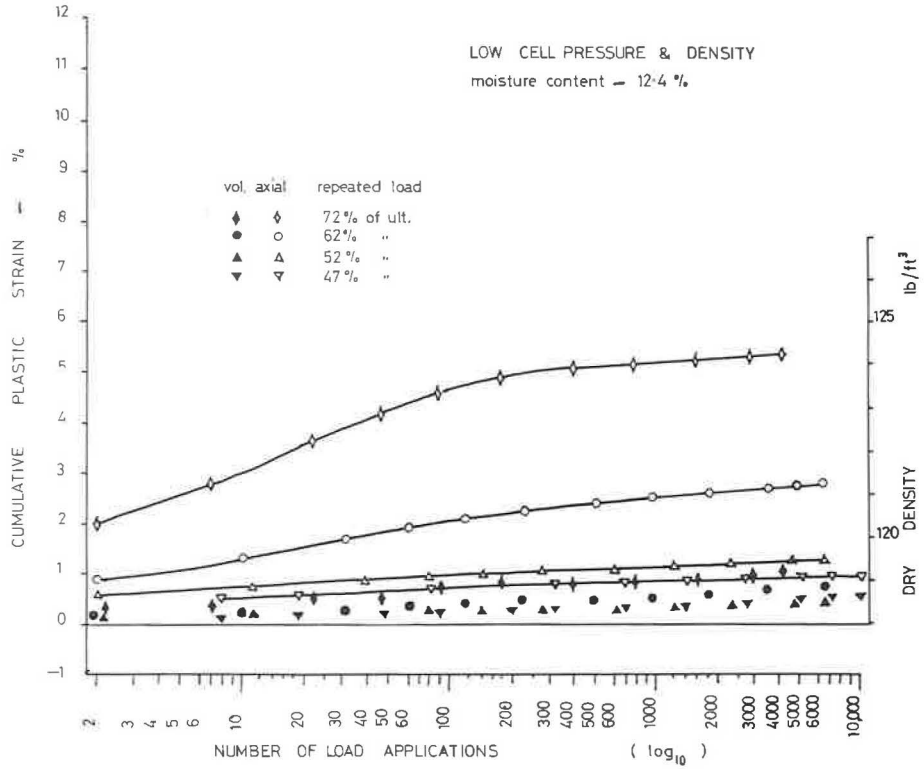

Figure 2. Cumulative plastic strain versus number of load applications applied to the unsaturated sample with a cell pressure of 5 psi.

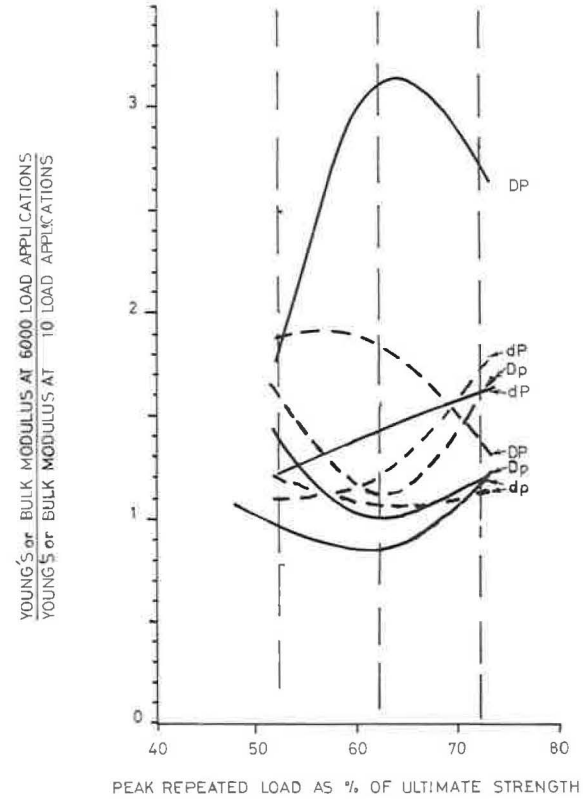

Figure 3. Ratio of the Young's or bulk modulus after 6,000 load applications over that after 10 applications versus the magnitude of repeated loads.

have produced more elastic bonds and hence a lower damping factor.

The author has shown (4) that the damping properties are a function of the average internal friction of the soil. This friction could stem from the bond making and braking, from pore fluid flow, or from the "Coulomb friction" of grain rubbing grain. It has been subsequently shown (6) that sand grains in the test soil do break up after a large number of repeated loadings presumably because of the grains rubbing together.

When the moisture content of a sample was gradually increased from 12 to 13 percent during a repeated loading test, the Young's modulus decreased and the damping factor and plastic strain increased. Some of the hysteresis loops are shown in Figures 5 and 6.

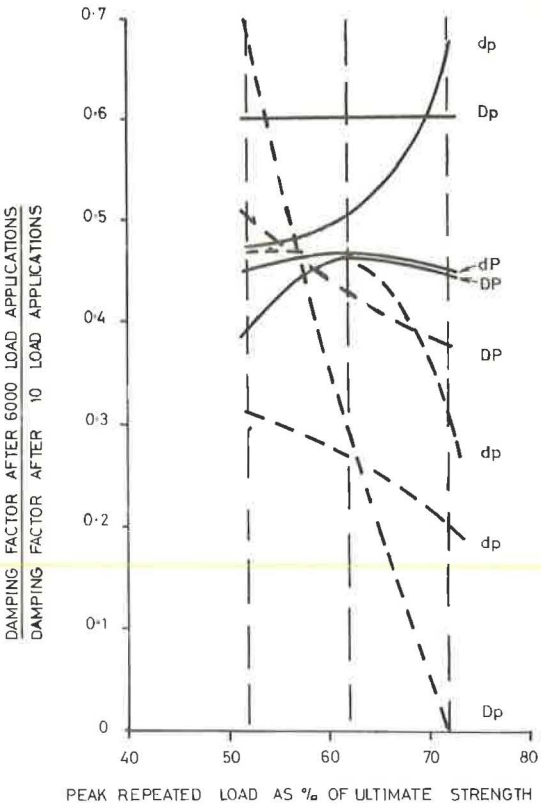

Figure 4. Ratio of the damping factor after 6,000 load applications over that after 10 applications versus the magnitude of repeated loads.

SEPARATION OF PLASTIC BEHAVIOR

Figure 7 shows the axial stress-strain hysteresis loops at the 17th and 10,309th application of load to an unsaturated sample with a low cell pressure (the volumetric behavior is shown in Figure 8). The commencement of each loop is reoriented to a common point to facilitate comparison.

It will be noted that even the loop for the 17th load application shows a large plastic strain. In fact, part of the area of the loop (which is large on the first load cycle and decreases with subsequent cycles) can be ascribed to plastic deformation. Figure 9 shows a typical and realistic hysteresis loop from an elastoplastic soil containing no elastic hysteresis and in which the change in plastic strain per unit absolute change in instantaneous stress is a function of the absolute instantaneous cycling stress. A loop containing the elastic as well as the plastic damping energy is shown by the broken line in Figure 10.

A theoretical method will now be described to demonstrate the elastoplastic behavior of a soil comprising a repeatedly rolled pavement. For clarity the characteristics of the material were assumed, contrary to the preceding test findings, to remain as they were on the first load cycles.

THE MECHANO-LATTICE ANALOGY

Elastoplastic Behavior

The author's mechano-lattice analogy described elsewhere (1, 2, 3) was used for the prediction of stress-strain behavior of an elastoplastic soil in a hypothetical pavement being subjected to repeated rolling. Only the elastoplastic components, as in the soil described previously, were used and were considered to have constant characteristics throughout the repeated rolling. For clarity, the elasto-frictional components (1) were ignored.

Figure 10 shows the elastoplastic components of the axial load versus deflection hysteresis loop recorded during a typical first or second load cycle. It will be noted that

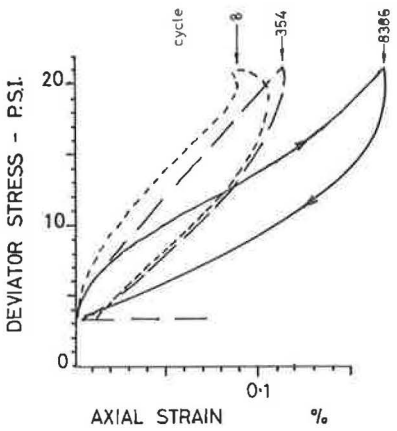

Figure 5. Axial stress-strain hysteresis loops for the 8th, 354th, and 8,386th cycles of a 47 percent of ultimate load on the unsaturated sample with a cell pressure of 5 psi as the moisture content increased from 12 to 13 percent, a dry density of 118 lb/ft^3, and a 47 percent of ultimate load.

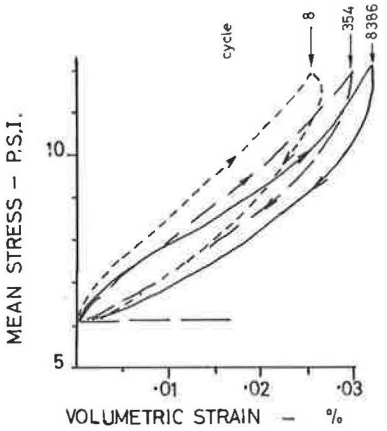

Figure 6. Volumetric stress-strain hysteresis loops for the 8th, 354th, and 8,386th cycles of a 47 percent of ultimate load on the unsaturated sample with a cell pressure of 5 psi as the moisture content increased from 12 to 13 percent.

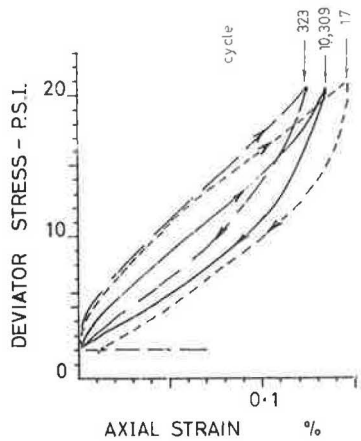

Figure 7. Axial stress-strain hysteresis loops for the 17th and 10,309th cycles of a 47 percent of ultimate load on the unsaturated sample with a cell pressure of 5 psi, a moisture content of 12.4 percent, and a dry density of 118 lb/ft^3.

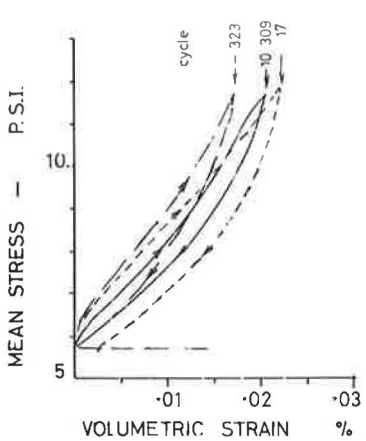

Figure 8. Volumetric stress-strain hysteresis loops for the 17th and 10,309th cycles of a 47 percent of ultimate load on the unsaturated sample with a cell pressure of 5 psi.

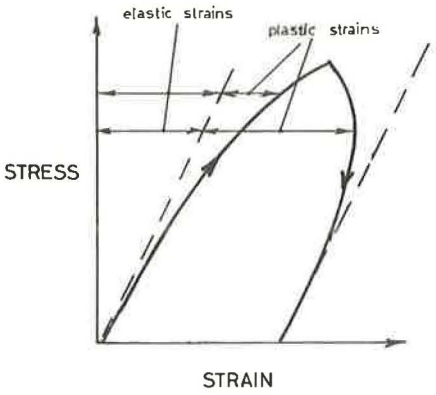

Figure 9. The axial stress-strain hysteresis loop of a hypothetical elastoplastic soil.

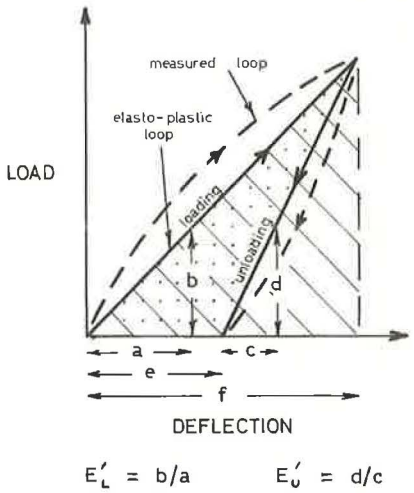

$E'_L = b/a$ $E'_U = d/c$

Figure 10. The simplification and partition of an axial elastoplastic load-deflection hysteresis loop from a measured loop.

a further simplification was made beyond that shown in Figure 9. The change in plastic deformation per unit absolute change in instantaneous load was assumed to be independent of instantaneous load and proportional instead to the mean absolute cycling load for one cycle. This produced a scalene-triangel shaped open loop that is more mathematically tractable.

The axial behavior can be considered as that of an elastic element that has a greater modulus when unloading, E_U, than when loading, E_L (Fig. 10). The plastic factor is e/f and is equal to the damping factor, ξ, which is the dotted area in the loop divided by the hatched area under the loading line.

Similar behavior will be ascribed to individual elements making up each two-dimensional unit of the analogy. The analogy simulates a long section of a pavement suffering plane stress (Fig. 11).

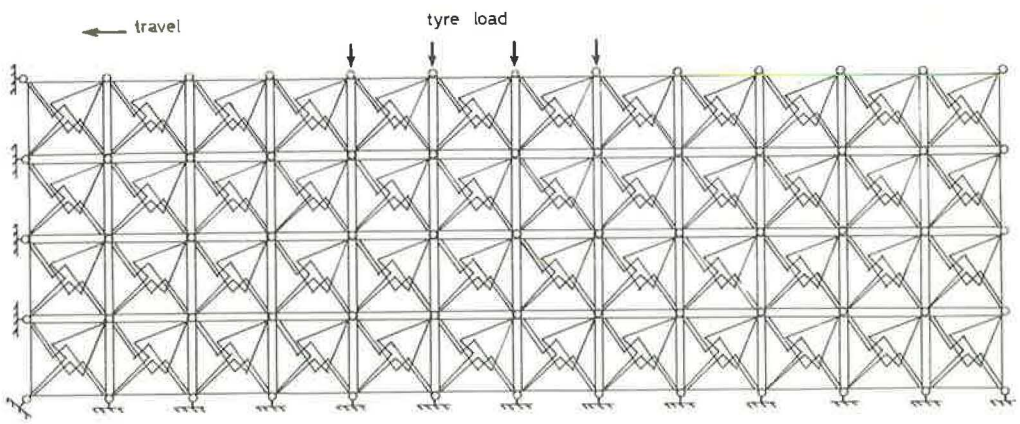

Figure 11. An assembly of units to simulate a long section of an elastoplastic pavement experiencing plane stress.

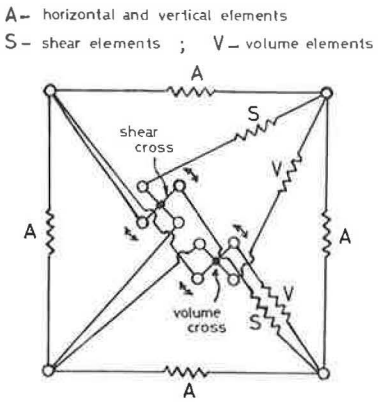

Figure 12. A unit of the lattice structure simulating the behavior of the soil.

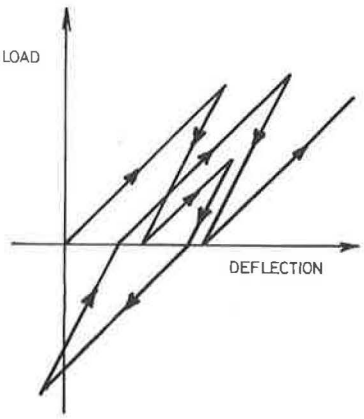

Figure 13. Possible load-deflection behavior of an element or model.

Plane Stress Simulation Unit of the Analogy

A diagram of the model unit is shown in Figure 12. The elastic elements exhibit one stiffness when the absolute load is increasing and a higher stiffness when the absolute load is decreasing. This produces plastic deformations that are not time-dependent. A possible load-deflection path exhibited by an element is shown in Figure 13. When a positive or negative unloading path crosses the deflection axis, it becomes a loading path and hence its slope decreases as shown.

Figure 10 shows the load-deflection path of one positive load cycle on any element. The slope of the loading path is equal to the loading stiffness coefficient, E'_L, of the element. The slope of the unloading path is E'_U. The damping energy per cycle is represented by the area in the loop. The damping factor is the area in the loop divided by the hatched area. The plastic factor is the plastic strain divided by the total strain.

The model shown in Figure 12 simulates the behavior of a material with a particular rigidity, plasticity, and Poisson's ratio. The two crosses, free to rotate, enable shear and volumetric behavior to be independent and thus allow various Poisson's ratios to be simulated. The left-hand cross permits the shear elements to be activated only when shear deformation is taking place. The right-hand cross permits the volume elements to be activated only during volume changes.

The stiffness coefficients of the elements are calculated by frame analysis for the representation of a non-buckling plate of unit thickness (7):

$$E'(\text{L or U}) = \frac{E_{(\text{L or U})}D}{2(1+\sigma)} \qquad \text{(horizontal and vertical elements)}$$

$$= \frac{E_{(\text{L or U})}D}{(a+\sigma)\sqrt{2}} \qquad \text{(the two shear elements)}$$

$$= \frac{E_{(\text{L or U})}D}{1-\sigma^2} \qquad \text{(the two volume elements)}$$

where

$E(\text{L or U})$ = Young's loading or unloading modulus
D = The length of a side of the model
σ = Poisson's ratio.

The complex case of a roller moving on an elastoplastic material is solved by connecting a number of models (Fig. 12) at their joints, as shown in Figure 11 to represent

a long section of road. The left-hand and base joints are fixed, and the right-hand and upper joints are free to move. A drum roller effect is represented by displacements to the central upper surface joints conforming to its radius. A pneumatic tire effect is produced by placing fixed loads on a number of the central upper joints.

SOLUTIONS

Solutions are achieved by an iterative procedure and by using an electronic digital computer. The program flow chart is shown in Figure 14. The force history of each element is traced by its consecutive changes in length and by its load. At the beginning of each calculation cycle the lengths of all elements, measured from joint to joint, are computed.

Stages in the cycles of load-deflection that an element experiences as the wheel rolls from right to left are represented by the states of corresponding elements examined in turn while moving from left to right in the same row. Thus the load-deflection path or hysteresis loop of each element is started from fixed values on the left and traced from one unit to the next by comparing compressions and elongations.

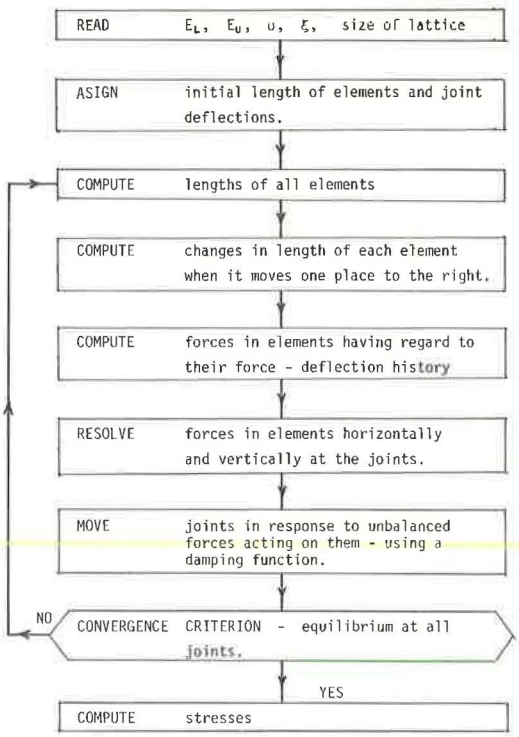

Figure 14. Flow diagram of the computer program.

If one element is shorter than the corresponding element in the model on the left, an increase in compressive loading is indicated when both elements have compressive loads. The change in length is multiplied by the element's stiffness coefficient, E'_L, to obtain the increase in load. The change in load in the element is added to its original load. When a load-deflection path crosses a line of zero load as the absolute load is decreasing, the stiffness coefficient is changed from E'_U to E'_L. Thus closed hysteresis loops can occur if the load is reversed. The foregoing process of computing the forces in all the elements is repeated for each element while moving along the rows.

The forces in the elements are next resolved horizontally and vertically at the adjacent joints. Each joint is then moved in the direction of those unbalanced forces by an amount that is a function of them.

This process of calculating lengths, changes in length, forces in elements, and movements of joints is repeated until convergence at about 150 cycles for 120 joints. Upon convergence, when the joints are in equilibrium, the stresses at the center of each model are calculated by averaging and resolving the forces in the appropriate elements.

For the solution of the second pass, the rectilinear and horizontally homogeneous residual stresses and strains following the first pass of the roller or wheel are ascribed to all the material at the start of second-pass calculations. In this way any number of repeated rollings can be simulated. In the present example only six passes were needed to achieve a constant residual stress distribution.

RESULTS

A hypothetical elastoplastic pavement 15 in. long and 2 in. thick resting on a rigid base was analyzed. It was, in simulation, repeatedly rolled by (a) a 40-in. diameter rigid roller and (b) a pneumatic tire. A loading modulus, E_L, of 5,000 psi; an unloading

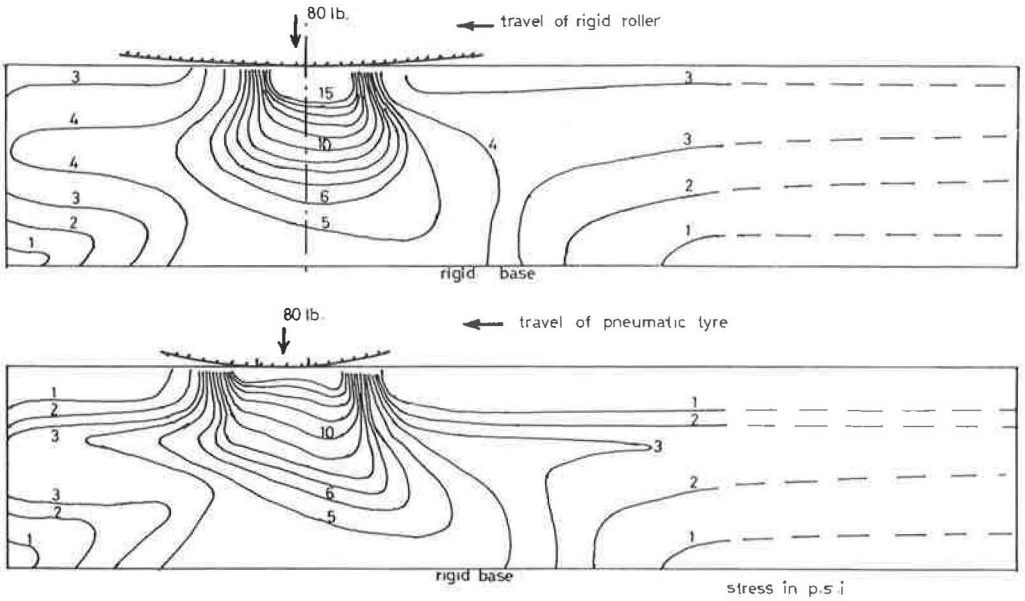

Figure 15. Transient and residual maximum shear stress patterns calculated during the 6th pass of the rigid roller and of the pneumatic tire.

modulus, E_U, of 10,000 psi; a Poisson's ratio, σ, of 0.4; and a damping and plastic factor of 0.5 were assumed.

Residual Stresses

Figure 15 shows the maximum shear stress distributions involved by the sixth passes of the roller and of the pneumatic tire respectively. The sum of the transient stresses, which moved with the load, and the residual stresses is shown in full lines. The residual stresses that remained are shown by broken lines. Although the loads were similar, the roller induced more intense stresses, especially forward of the moving load.

The buildup of residual stresses during repeated rolling is one of the most important properties of elastoplastic road materials. In the present problem the horizontal residual stresses increased at a reducing rate until they became constant after the sixth pass (Fig. 16).

The distribution with depth of the horizontal and vertical residual stresses re-resulting from the repeated passing of the rigid roller and the pneumatic tire are shown in Figure 17. In each case the vertical residual stress was small and tensile and changed little with the number of passes. The vertical residual tensile stress would be partly offset by the neglected weight of the road material.

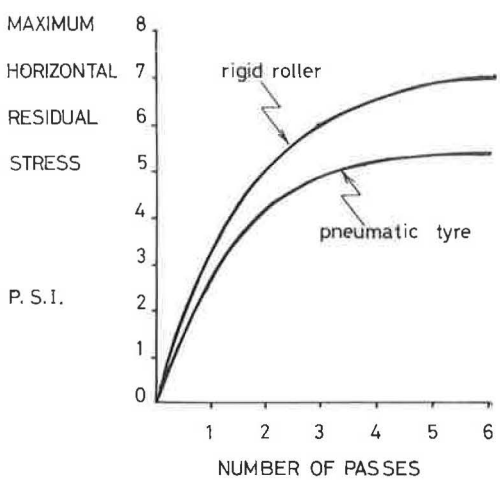

Figure 16. Maximum horizontal residual stresses versus number of passes.

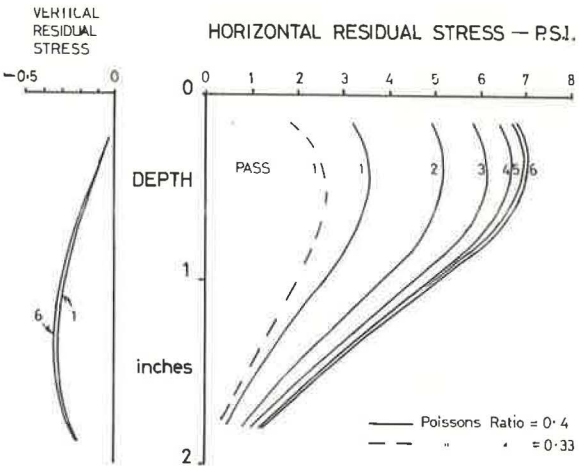

(a) Rigid Roller

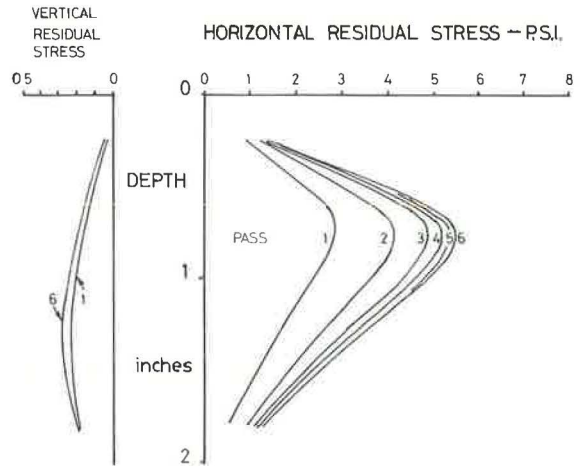

(b) Pneumatic Tyre

Figure 17. Residual stress distribution with depth.

The roller caused the maximum horizontal residual stress to build up close to the surface, whereas the pneumatic tire caused this maximum to occur well below the surface, leaving the surface unstressed. The rigid roller induced greater residual stresses. Increasing the Poisson's ratio increased the residual stresses; i.e., greater residual stresses would occur in well-compacted or highly saturated materials if other factors are constant.

The rolling resistance of the rigid roller was calculated from the torque produced by the nonsymmetrical reactions at the surface of contact—that of the tire from the uphill slope of the surface of contact. In both cases the rolling resistance decreased at a low rate as passes continued. The roller had the greater resistance to rolling (Fig. 18).

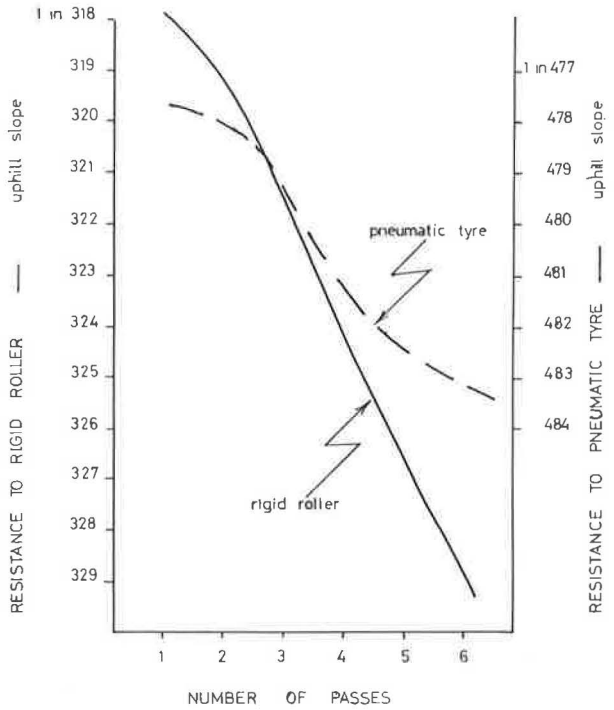

Figure 18. Rolling resistance.

Cumulative Strains

If this hypothetical road material were to lose its plastic hysteresis after a large number of passes—as it usually does in practice—the surface deformation would become symmetrical, and the pavement would lose its resistance to rolling because no elastic hysteresis was present. The vertical plastic and elastic strains per pass remained constant.

The horizontal flow that varied with depth caused complex shear behavior. There was a marked difference in shear behavior between that induced by the roller and that induced by the pneumatic tire, as is evident in Figure 19, which shows the cumulative horizontal flow at each depth.

The roller induced a very marked forward permanent shear in the top layer that continued with the number of passes. The lower layer also sheared forward, whereas the intermediate layers sheared slightly backward. The whole body of the soil moved steadily forward (against the direction of rolling). The phenomenon of forward shear was shown by Hamilton (8) to exist in repeatedly rolled copper. Merwin and Johnson (9) used approximate estimates based on the Hertz distribution to check Hamilton's findings.

In contrast the simulated pneumatic tire induced a backward shear in the top layer, while the deeper soil sheared forward. The body of material moved forward at a greater rate than when the similarly loaded roller was passing.

Whether the greater forward shear associated with rigid rolling causes disruption at the surface or aids in compaction must depend on the nature of the road material.

QUALITATIVE VERIFICATION OF THE THEORETICAL FLOW PREDICTIONS

The theoretically predicted cumulative deformational behavior of the hypothetical elastoplastic road material was qualitatively checked with practice. This was done by

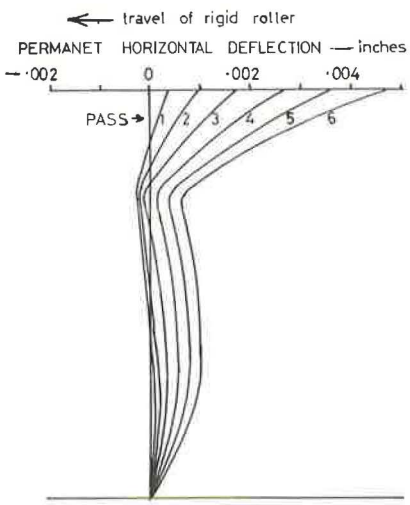

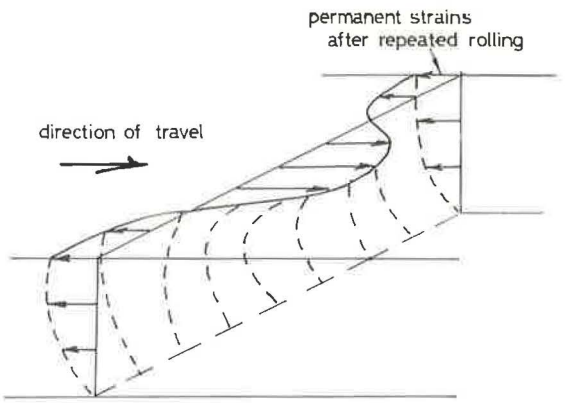

Figure 20. The measured and estimated horizontal flow pattern in Sparks and Davis test track.

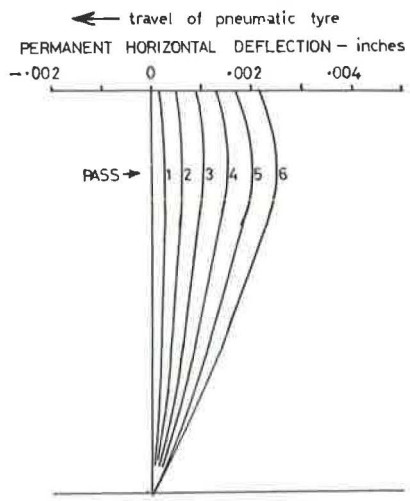

Figure 19. Horizontal flow of material at each depth.

repeatedly rolling a 2-in. diameter roller on a two-colored layer of modeling clay ½ in. thick. A vertical plane was formed at the interface of the two colors so that flows could be observed.

When the roller was torque driven, as with the theoretical examples, the flow was against the direction of rolling as predicted. When the roller was moved by a horizontal force applied at the axle, the flow was against the direction of travel in the body of material but the surface layer was moved differentially back in the direction of the roller travel.

Subsequent to the work described here, Sparks and Davis (10) used a loaded, free-running pneumatic tire repeatedly rolling in the one direction on the central third of a long straight test track. The 6-in. thick test pavement consisted of $^{3}/_{16}$ in. to dust size crushed dolerite, 10 percent kaolinite binder, and a moisture content of 5½ percent. After a large number of passes, the surface of that part of the track rolled by the tire moved in the direction of travel, while the outer nontraversed parts moved against the direction of travel, as shown by the full line in Figure 20. The shape of an initially vertical plane is shown by broken lines. Its subsurface shape is this author's estimate based on the foregoing theoretical work and the laboratory tests with modeling clay.

CONCLUSION

The repeated load soil tests described here have shed light on energy and flow characteristics of road materials. At least one type of material undergoes great changes in damping factor, stiffness, and plasticity while being either repeatedly or constantly loaded. It was shown that a small change in moisture content can drastically change the values of the foregoing characteristics from safe levels.

The theoretical analysis and confirming practical proof described assumed that the values of the material stiffness and plastic and damping characteristics of a pavement

were constant throughout repeated traverses by loaded wheels or rollers. It was shown that the pavement material flows in the opposite direction to the traffic movement. The differential of the distribution of the material flow with depth may lead to some type of surface contortion and hence to failure. When the road material properties vary from location to location, the changes in flow rate may lead to the surface uneveness that renders a road unservicable. The theoretically demonstrated horizontal residual stresses could lead to buckling and perhaps corrugations of the surface.

As shown by the repeated-load triaxial tests on soil, plasticity almost disappears after a large number of load applications; in this case the flow and associated contortion of the road surface comprising the soil would cease to worsen. In the case of the earth pavement, however, an increase in moisture content can, as previously shown, reestablish plastic flow. In the case of bitumen roads, an increase in temperature can also reestablish plastic flows and further surface irregularities would appear.

ACKNOWLEDGMENT

The author wishes to thank Professor D. F. Orchard for his encouragement.

REFERENCES

1. Yandell, W. O. Stress Distribution Associated With Rolling Resistance. Australian Road Research, Vol. 3, No. 1, March 1967, pp. 3-13.
2. Yandell, W. O. Rolling Resistance and Stress Distribution Associated With Plastic Hysteresis. Inst. of Engrs. Aust. Jour. Paper No. 2370, Oct.-Nov. 1967, p. 179.
3. Yandell, W. O. The Effect of Repeated Rolling of Elastoplastic Roads. Australian Road Research, Vol. 3, No. 7, Sept. 1968, pp. 3-13.
4. Yandell, W. O. The Effect of Repeated Loading on Road Making Materials. M.E. thesis, University of New South Wales, 1966.
5. Yandell, W.O. Some Effects of Repeated Loads. Proc. Third Conf. of Australian Road Research Board, Sydney, Sept. 4-5, 1966. A.R.R.B., Vol. 3, Part 2, (paper 279), 1967, pp. 1100-17.
6. Shackel, B. Private communication, 1970.
7. McHenry, D. A Lattice Analogy for the Solution of Stress Problems. Jour. I.C.E., Vol. 21, No. 2, (paper 5350) Dec 1943, pp. 59-82.
8. Hamilton, G. M. Plastic Flow in Rollers Loaded Beyond the Yield Point. Proc. Inst. Mech. Engr., Vol. 177, No. 25, (Appl. Mech. Group Paper), 1963, pp. 667-75.
9. Merwin, J. E., and Johnson, K. L. An Analysis of Plastic Deformation in Rolling Contact. Proc. Inst. Mech. Engr., Vol. 177, No. 25, (Appl. Mech. Group Paper), 1963, pp. 676-85.
10. Sparks, G. H., and Davis, E. H. First Road Base Experiment With a Laboratory Test Track. A.R.R.B., 5th Conf., August 1970.